Phase-Anchored SC-OFDM

Fumihiro Hasegawa, Masatsugu Higashinaka, Akihiro Okazaki, Fumio Ishizu,
Damien Castelain, Loïc Brunel, and David Mottier

***Abstract*—A new out-of-band power suppression method for single carrier (SC)-orthogonal frequency division multiplexing (OFDM) is proposed in this letter. In the proposed method, by inserting two static "anchor symbols" at designated positions in every SC-OFDM block, phase continuity between SC-OFDM blocks is preserved and out-of-band power emissions are reduced without bit error rate (BER) performance degradation. Both experimental and simulation results indicate that reduction of out-of-band emissions up to 13dB can be achieved by using the proposed method.**

***Index Terms*—SC-OFDM, out-of-band emissions**

I. Introduction

SINGLE CARRIER-orthogonal frequency division multiplexing (OFDM) is an attractive block transmission method due to its low peak power and robust performance against multipath fading channels [1]. However, phase discontinuity exists between single carrier (SC)-OFDM blocks and out-of-band emissions, which is a well-known concern in OFDM [2], becomes a critical problem. Windowing techniques [3] can be implemented to create phase continuity between SC-OFDM blocks, but they reduce the effective length of cyclic prefix (CP).

In the proposed scheme, "anchor symbols", which are used to "anchor" phases of the first and last sample of each SC-OFDM block, are inserted at predetermined positions to maintain phase continuity between blocks and to reduce out-of-band emissions. It will be shown in this letter that the proposed scheme can be easily adapted for data and pilot multiplexed SC-OFDM blocks described in [4].

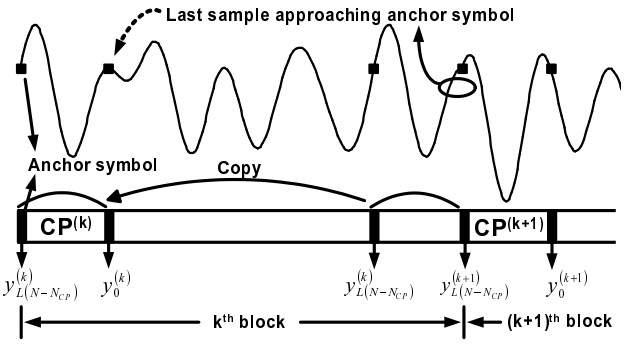

Fig. 1. Phase continuity due to anchor symbols between SC-OFDM blocks

F. Hasegawa, M. Higashinaka, A. Okazaki and F. Ishizu are with Mitsubishi Electric Corporation, Information Technology R & D Center, Kamakura, Kanagawa 247-8501, Japan. (e-mail: Hasegawa.Fumihiro@bk.MitsubishiElectric.co.jp).

D. Castelain, L. Brunel and D. Mottier are with Mitsubishi Electric R&D Centre Europe, CS 10806, 35708 Rennes Cedex 7, France.

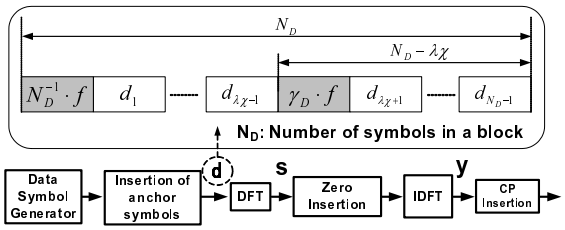

Fig. 2. Block diagram of the proposed SC-OFDM transmitter

II. Proposed SC-OFDM Transmission Schemes

A. Data only SC-OFDM

In this subsection, signal design for a SC-OFDM block consisting of only data symbols is described. Let us define N, N_A, N_D and N_{CP} as the number of symbols, active subcarriers, data symbols and length of CP, respectively. First, N_D information symbols $\mathbf{d}^{(k)} = \left[d_0^{(k)}, \cdots, d_{N_D-1}^{(k)}\right]^T$ for the k^{th} block are precoded by the $N_D \times N_D$ discrete Fourier transform (DFT) matrix: $\mathbf{s}^{(k)} = \left[s_0^{(k)}, \cdots, s_{N_D-1}^{(k)}\right]^T = \mathbf{W}_{N_D}\mathbf{d}^{(k)}$. The $(k,l)^{th}$ element of the $N \times N$ DFT matrix $\mathbf{W}_N$ is given by $[\mathbf{W}_N]_{k,l} = \frac{1}{\sqrt{N}} e^{-j2\pi kl/N}$. Assuming both N and N_D are even numbers, the DFT precoded symbols $\mathbf{s}$ are mapped onto $N_A = N_D$ subcarriers as follows, $\mathbf{v}^{(k)} = \left[v_0^{(k)}, \cdots, v_{N-1}^{(k)}\right]^T = \left[\mathbf{0}_{1,(N-N_A)/2}, \mathbf{s}^{(k)T}, \mathbf{0}_{1,(N-N_A)/2}\right]^T$, where $\mathbf{0}_{N,M}$ is an all-zero $N \times M$ matrix. The output of the inverse discrete Fourier transform (IDFT) corresponding to the k^{th} block, which contains N data symbols oversampled L times by zero-padding in the frequency domain (FD), is written as $\mathbf{y}^{(k)} = \left[y_0^{(k)}, \cdots, y_{NL-1}^{(k)}\right]^T$. The last LN_{CP} samples of $\mathbf{y}^{(k)}$, denoted as $\mathbf{y}_{CP}^{(k)} = \left[y_{L(N-N_{CP})}^{(k)}, y_{L(N-N_{CP})+1}^{(k)}, \cdots, y_{NL-1}^{(k)}\right]^T$, are used as CP. Thus, the transmitted signal can be written as $\mathbf{y}^{(k)'} = [\mathbf{y}_{CP}^{(k)T}, \mathbf{y}^{(k)T}]^T$. Rewriting the output of IDFT [1], it can be shown that the $(L \cdot n)^{th}$ element of $\mathbf{y}^{(k)}$ can be expressed as

$$y_{Ln}^{(k)} = e^{j\pi n\left(L-\frac{N_D}{N}\right)} \sum_{m=0}^{N_D-1} d_m^{(k)} \sum_{l=0}^{N_D-1} e^{j2\pi l\left(\frac{n}{N}-\frac{m}{N_D}\right)}, \quad (1)$$

for $0 \le n \le N-1$. For simplicity, a normalization constant is omitted from (1). If we define c as an arbitrary constant, phase continuity between SC-OFDM blocks can be maintained by inserting anchor symbols at the following positions:

- R1: The first symbol of an SC-OFDM block contains the anchor symbol f, i.e., $y_0^{(k)} = f = c \cdot d_0^{(k)}$,
- R2: The first sample of the CP of an SC-OFDM block is the anchor symbol f, i.e., $y_{L(N-N_{CP})}^{(k)} = f$

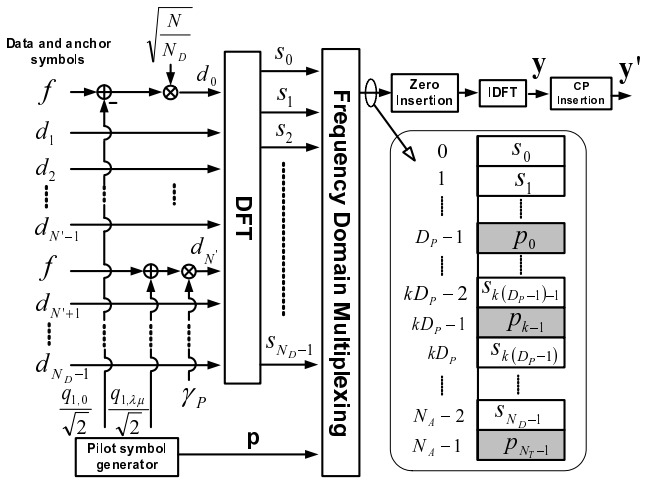

Fig. 3. Block diagram of the transmitter for hybrid SC-OFDM transmission

The goal here is to maintain phase continuity between the last sample of the k^{th} block $y_{LN-1}^{(k)}$ and first sample of the $k+1^{th}$ block $y_{L(N-N_{CP})}^{(k+1)}$. As shown in Fig. 1, due to the periodic extension of the zero-padded signal at the output of IDFT [5, pp. 107], phase of $y_{LN-1}^{(k)}$ approaches that of the first symbol $d_0^{(k)} = f$ according to R1. Thanks to R2, the first sample of the CP of the next block, $y_{L(N-N_{CP})}^{(k+1)}$ is also the anchor symbol, preserving phase continuity between $y_{LN-1}^{(k)}$ and $y_{L(N-N_{CP})}^{(k+1)}$.

According to R2, the first sample of the CP $y_{L(N-N_{CP})}^{(k)}$ must be the anchor symbol without any intersymbol interference. Let us define integers χ and μ, which determine the position of the anchor symbol in the data block and at the output of IDFT, respectively. Let us also define a constant λ with $0 \leq \lambda \leq N/\mu - 1$. If μ and χ satisfy the following equation,

$$\frac{\mu}{N} = \frac{\chi}{N_D}, \tag{2}$$

by substituting $\lambda\mu$ and $\lambda\chi$ in n and m respectively in (1), it can be shown that $y_{L\lambda\mu}^{(k)} = N_D \cdot e^{j\pi\lambda(L\mu-\chi)} \cdot d_{\lambda\chi}^{(k)}$. Equivalently, if the anchor symbol is placed at the $\lambda\chi^{th}$ symbol in the data block, it appears at the $L\lambda\mu^{th}$ sample at the output of IDFT without intersymbol interference. Consequently, the length of CP can be determined by $N_{CP} = N - \lambda\mu$. Finally, to satisfy both R1 and R2, the anchor symbols can be placed as follows,

$$d_m^{(k)} = \begin{cases} N_D^{-1} \cdot f & m = 0 \\ \gamma_D \cdot f & m = \lambda\chi \end{cases} \tag{3}$$

where $\gamma_D = N_D^{-1} e^{-j\pi\lambda(L\mu-\chi)}$. As shown in Fig. 2, a block of $N_D - 2$ data symbols d_i are generated for each SC-OFDM block and anchor symbols are placed as specified in (3) in the proposed scheme. It should be noted that the loss in spectral efficiency becomes $\eta = \frac{2}{N_A}$ in the proposed scheme.

B. Pilot and data symbol multiplexed SC-OFDM

1) Placement of anchor symbols: In [4], pilot and data multiplexed "hybrid" SC-OFDM signalling was proposed to improve channel estimation performance in time-varying fading channels. In this subsection, the proposed scheme is modified for the hybrid SC-OFDM transmission. By defining N' as the location of the second anchor symbol, the proposed hybrid SC-OFDM transmission scheme is shown in Fig. 3. An arrangement of hybrid and data-only SC-OFDM blocks in a data frame is shown in Fig. 4. As shown in Fig. 4, N_T pilot symbols are placed in the FD at indices $I_T = \{D_P - 1, 2D_P - 1, \cdots, N_A - 1\}$ with $D_P = N_A/N_T$ where $N_A = N_D + N_T$, and hybrid blocks are separated by T_D data blocks in the time domain (TD). A data frame contains F data and hybrid SC-OFDM blocks and N_T is assumed to be an even number. The data indices in the FD are given by $k \in I_D$ where I_D contains integer values between 0 and $N_A - 1$ and not belonging to I_T.

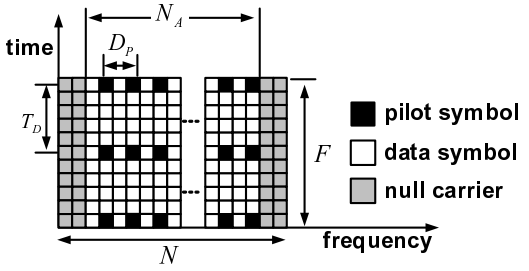

Fig. 4. Frame structure

Let us define an $N_A \times N_D$ placement matrix for DFT precoded data symbols as $[\mathbf{P}_D]_{k,l} = 1$ if $k \in I_D$ and $l = k - \lfloor k/D_P \rfloor$, and $[\mathbf{P}_D]_{k,l} = 0$ otherwise. Let us also define an $N_A \times N_T$ pilot symbol placement matrix with $[\mathbf{P}_T]_{k,l} = 1$ if $l = \lfloor k/D_P \rfloor$ and $[\mathbf{P}_T]_{k,l} = 0$ otherwise. The pilot symbols in the FD are denoted as $\mathbf{p} = [p_0, \cdots, p_{N_T-1}]^T$. In this letter, the following Zadoff-Chu (ZC) sequence [4],

$$p_{k,P_Z} = e^{\frac{-j\pi}{N_T}\left(P_Z k^2 + k\right)} \qquad 0 \leq k \leq N_T - 1 \tag{4}$$

parameterized by P_Z is used as a pilot sequence. Let us define $N_Z = (N - N_A)/2$. Then, the pilot-data multiplexed signal in the FD can be represented as $\mathbf{v}^{(k)} = \left[\mathbf{0}_{1,N_Z}, \left(\mathbf{P}_D \mathbf{W}_{N_D} \mathbf{d}^{(k)} + \mathbf{P}_T \mathbf{p}\right)^T, \mathbf{0}_{1,N_Z}\right]^T$. Without the loss of generality, a non-oversampled model is considered in this section. The non-oversampled output of the IDFT $\mathbf{x}^{(k)} = \left[x_0^{(k)}, \cdots, x_{N-1}^{(k)}\right]^T$ is given by,

$$\mathbf{x}^{(k)} = \underbrace{\mathbf{W}_N^H \begin{bmatrix} \mathbf{0}_{N_Z,N_D} \\ \mathbf{P}_D \mathbf{W}_{N_D} \\ \mathbf{0}_{N_Z,N_D} \end{bmatrix}}_{\mathbf{A}_{N,N_D}} \mathbf{d}^{(k)} + \underbrace{\mathbf{W}_N^H \begin{bmatrix} \mathbf{0}_{N_Z,1} \\ \mathbf{P}_T \mathbf{p} \\ \mathbf{0}_{N_Z,1} \end{bmatrix}}_{\mathbf{q}} \tag{5}$$

In this letter, it is assumed that $N_D = N_T$ since the peak to average power ratio (PAPR) of the hybrid SC-OFDM block can be minimized when $N_D = N_T$, as described in [4]. Let us assume that $N_Z/2$ is an integer. Then, defining a diagonal phase rotation matrix $\mathbf{\Phi} = \text{diag}\left\{1, \cdots, e^{j2\pi \cdot n/N}, \cdots, e^{\frac{j2\pi}{N} \cdot \left(\frac{N}{2}-1\right)}\right\}$ and $\mathbf{q}_1 = \left[q_{1,0}, \cdots, q_{1,N/2-1}\right]^T = \mathbf{\Phi} \mathbf{W}_{N/2}^H \left[\mathbf{0}_{1,N_Z/2}, \mathbf{p}^T, \mathbf{0}_{1,N_Z/2}\right]^T$,

TABLE I
THRESHOLD δ TO REACH CCDF (INP(δ)) $= 10^{-2}$ FOR $\mathbf{x}_Z$, QPSK, $N = 64$, $N_D = N_T = 28$, $N_{CP} = 8$, $f = \frac{1-j}{\sqrt{2}}$

P_Z	1	3	5	9	15	17	23	27
δ (dB)	2.33	7.38	5.33	5.00	6.31	6.97	6.4	7.8

the pilot symbols in the TD can be expressed as

$$\mathbf{q} = \frac{1}{\sqrt{2}} \left[\mathbf{q}_1^T, -\mathbf{q}_1^T\right]^T. \quad (6)$$

Denoting $\mathbf{d}_1^{(k)} = \mathbf{W}_{N/2}^H \left[\mathbf{0}_{1,N_Z/2}, \left(\mathbf{W}_{N_D}\mathbf{d}^{(k)}\right)^T, \mathbf{0}_{1,N_Z/2}\right]^T$ and $\mathbf{d}_1^{(k)} = \left[d_{1,0}^{(k)}, \cdots, d_{1,N/2-1}^{(k)}\right]^T$, it can be shown that

$$\mathbf{A}_{N,N_D}\mathbf{d}^{(k)} = \frac{1}{\sqrt{2}} \left[\mathbf{d}_1^{(k)T}, \mathbf{d}_1^{(k)T}\right]^T. \quad (7)$$

When $N_D = N_T$, it is clear from (6) and (7) that inter-symbol interference does not exist and only pilot symbols in the TD can be considered when designing anchor symbols for hybrid SC-OFDM blocks. Furthermore, the n^{th} element of $\mathbf{d}_1^{(k)}$ can be written as follows,

$$d_{1,n}^{(k)} = \frac{e^{j\pi n\left(1-\frac{2N_D}{N}\right)}}{\sqrt{N_D \cdot N/2}} \sum_{m=0}^{N_D-1} d_m^{(k)} \sum_{l=0}^{N_D-1} e^{j2\pi l\left(\frac{2n}{N}-\frac{m}{N_D}\right)}, \quad (8)$$

for $0 \le n \le N/2-1$. From (8), if a pair of variables (μ, χ) satisfies the following equation,

$$\frac{2\mu}{N} = \frac{\chi}{N_D}, \quad (9)$$

it can be shown that $d_{1,\lambda\mu}^{(k)} = \sqrt{\frac{2N_D}{N}} e^{j\pi\lambda(\mu-\chi)} \cdot d_{\lambda\chi}^{(k)}$ for $0 \le \lambda \le N/(2\mu) - 1$. Thus, as shown in Fig. 3, anchor symbols f can be placed as follows to satisfy R1 and R2,

$$d_m^{(k)} = \begin{cases} \sqrt{\frac{N}{N_D}}\left(f - q_{1,0}/\sqrt{2}\right) & m = 0 \\ \gamma_P\left(f + q_{1,N/2-N_{CP}}/\sqrt{2}\right) & m = \lambda\chi \end{cases} \quad (10)$$

with $N_{CP} = N/2 - \lambda\mu$ and $\gamma_P = \sqrt{\frac{N}{N_D}} e^{-j\pi\lambda(\mu-\chi)}$.

2) Pilot Sequence Design: Due to the periodicity in both pilot (6) and data (7) signals, it can be shown that $x_{\lambda\mu}^{(k)}$ and $x_{N/2}^{(k)}$ are given by $x_{\lambda\mu}^{(k)} = f + \sqrt{2} \cdot q_{1,\lambda\mu} + \epsilon_{\lambda\mu}$ and $x_{N/2}^{(k)} = f - \sqrt{2} \cdot q_{1,0} + \epsilon_{N/2}$, respectively, where ϵ_i is a data-dependent term. From $x_{\lambda\mu}^{(k)}$ and $x_{N/2}^{(k)}$, it is clear that pilot signals $q_{1,\lambda\mu}$ and $q_{1,0}$ increase the peak power at $k' = \lambda\mu$ and $k' = N/2$, respectively. Thus, the pilot sequence $\mathbf{p}$ must be optimized to minimize the PAPR.

To optimize the PAPR performance of the hybrid SC-OFDM blocks, instantaneous normalized power (INP) performance of the hybrid SC-OFDM block without data symbols $\mathbf{x}_Z = \mathbf{A}_{N,N_D}\mathbf{d}_Z + \mathbf{q}$ is investigated. A vector of symbols $\mathbf{d}_Z$ which consists of pilot and anchor symbols is defined as, $d_{Z,0} = \sqrt{\frac{N}{N_D}}\left(f - q_{1,0}/\sqrt{2}\right)$, $d_{Z,\lambda\chi} = \gamma_P\left(f + q_{1,\lambda\mu}/\sqrt{2}\right)$ and $d_{Z,k} = 0$ if $k \ne \{0, \lambda\chi\}$. The complementary cumulative distribution function (CCDF) of INP, which is defined as $\text{CCDF}\left(\text{INP}(\delta)\right) = P\left(\frac{\left|y_n^{(k)}\right|^2}{E\left[\left|y_n^{(k)}\right|^2\right]} > \delta\right)$ [6], is investigated.

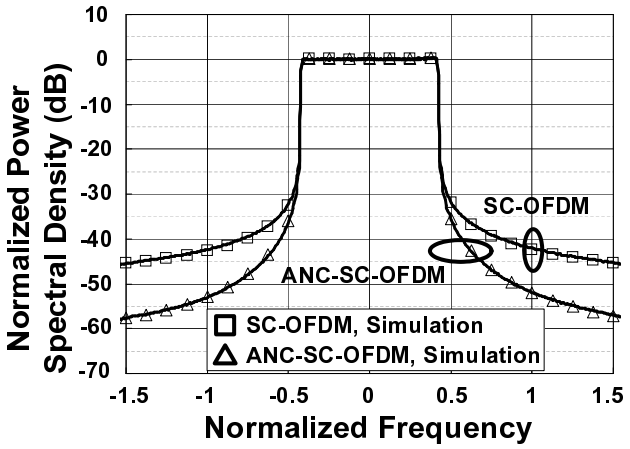

Fig. 5. Experimental and simulated power spectral density of the proposed transmission method with $N = 1024$, $N_A = 864$, $N_{CP} = 64$, $f = \frac{1+j}{\sqrt{2}}$, $P_Z = 1$, $L = 4$. Solid lines represent experimental results.

The pilot sequence is optimized by choosing a PAPR minimizing P_Z. Note that since N_T is assumed to be an even number, odd numbers are considered as candidates for P_Z such that $P_Z = \{1, 3, \cdots, N_T - 1\}$.

In Table I, INP performances of $\mathbf{x}_Z$ for quadrature phase shift keying (QPSK) and selected values of P_Z are shown. As an example, the parameters used in the simulation are set as $N = 64$, $N_T = N_D = 28$ and $f = \frac{1-j}{\sqrt{2}}$. The oversampling rate $L = 16$ is assumed. The thresholds δ to reach CCDF (INP(δ)) $= 10^{-2}$ for various values of P_Z are investigated. Since the parameters $\chi = 7$ and $\mu = 8$ satisfy both (2) and (9), the cyclic prefix length can be set as $N_{CP} = 8$ with $\lambda = 3$. It is clear from Table I that the lowest peak power can be obtained with $P_Z = 1$.

III. SIMULATION RESULTS

The power spectrum of the proposed method is shown in Fig. 5. Both simulated and experimental results are shown in the figure. In the simulation, a data frame with $T_D = 5$, $F = 41$, $N = 1024$, $N_A = 864$ and $N_{CP} = 64$ is assumed. In data-only and hybrid SC-OFDM blocks, the number of data symbols is set as $N_D = 864$ and $N_D = N_T = 432$, respectively. Note that the loss of data rate due to insertion of anchor symbols in this example is $\eta = \frac{2}{864} \approx 0.23\%$. The proposed anchor symbols shown in (3) and (10) are used in the comparison. In the experiment, signal bandwidth of 5MHz is assumed. Anritsu MG3700A and Anritsu MS2781B are used to generate waveforms and collect data, respectively. In the simulation, the spectrum is estimated with the Welch's averaged periodogram method with a NL sample-Hann window [5] and $NL/8$ overlap. The spectrum of SC-OFDM with anchor symbols (ANC-SC-OFDM) is shown in Fig. 5. Compared to the conventional SC-OFDM, it can be seen from the figure that the proposed scheme reduces the out-of-band emissions by almost 13dB.

The simulated INP performance for QPSK with P_Z obtained in Section II-B2 is shown in Fig. 6. As the performance benchmark, the INP performances of SC-OFDM and OFDM are

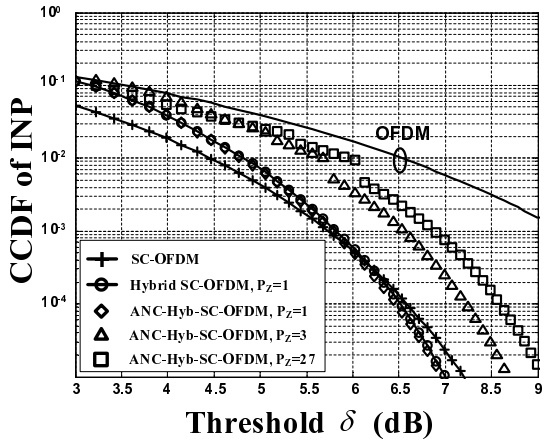

Fig. 6. CCDF of INP, $N = 64$, $N_D = N_T = 28$, $N_{CP} = 8$, $f = \frac{1-j}{\sqrt{2}}$

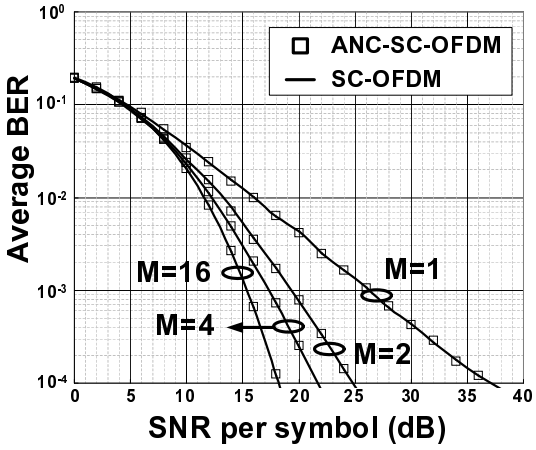

Fig. 7. Uncoded BER Performance, QPSK, $N = 512$, $N_A = 432$, $N_{CP} = 32$, $f = \frac{1+j}{\sqrt{2}}$, $P_Z = 215$

also shown in the figure. It is clear from the figure that the INP performance of the hybrid SC-OFDM with the proposed anchor symbols (ANC-Hyb-SC-OFDM) is equivalent to the INP performance of hybrid SC-OFDM [4]. The discontinuities in the INP curves for $P_Z = \{3, 27\}$ near CCDF $= 10^{-2}$ are caused by insertion of the anchor symbols.

Finally, the uncoded average bit error rate (BER) performances of the proposed scheme in Rayleigh frequency selective channels for QPSK with $T_D = 5$, $F = 21$, $N_A = 432$, $N = 512$, $N_{CP} = 32$ and $P_Z = 215$ are presented in Fig. 7. The number of data symbols is set as $N_D = 432$ and $N_D = N_T = 216$ in data-only and hybrid SC-OFDM blocks, respectively. In this letter, a Rayleigh frequency selective channel model $g(t) = \sum_{m=0}^{M-1} h_m \delta(t - mT_C)$ is considered where $T_S = N \cdot T_C$, $\delta(\cdot)$ and M denote the SC-OFDM block duration, delta function and number of multipaths, respectively. It is assumed that the channel remains constant during one SC-OFDM block interval and $E[h_l \cdot h_m^*] = \frac{1}{M}\delta(l-m)$ for $\forall l, m$ where the asterisk denotes the complex conjugate. If we denote the channel coefficients in the FD as $g_m^{(k)}$, the received signal in the FD can be represented by $r_m^{(k)} = g_m^{(k)} \cdot v_m^{(k)} + w_m^{(k)}$ where $E[|v_m^{(k)}|^2] = E_s$ and $w_m^{(k)}$ is additive white Gaussian noise (AWGN) with $E\left[|w_m^{(k)}|^2\right] = \sigma_w^2$ for $0 \le m \le N-1$.

The minimum mean square error (MMSE) equalizer is used where the equalization weights are given by $\zeta_m^{(k)} = \hat{g}_m^{(k)*} / \left(\left|\hat{g}_m^{(k)}\right|^2 + \sigma_w^2\right)$ for $0 \le m \le N-1$. The estimated channel coefficients are given by $\hat{g}_m^{(k)}$. If we define $[\mathbf{W}_{N,M}]_{m,n} = e^{-j2\pi mn/N}$ for $0 \le m \le N-1$ and $0 \le n \le L-1$, an estimate of the channel coefficients can be obtained with $\hat{\mathbf{g}}^{(k)} = \left[\hat{g}_0^{(k)}, \cdots, \hat{g}_{N-1}^{(k)}\right]^T = \mathbf{W}_{N,M}\left(\mathbf{W}_T^H \mathbf{W}_T\right)^{-1} \mathbf{W}_T^H \mathbf{S}_T^H \mathbf{r}_T^{(k)}$, where $\mathbf{W}_T$ is obtained by extracting rows that correspond to the locations of the pilot symbols from $\mathbf{W}_{N,L}$ and $\mathbf{S}_T = \text{diag}\{\mathbf{p}\}$. Similarly, $\mathbf{r}_T$ contains observations that correspond to the locations of the pilot symbols, extracted from the received signal, $\mathbf{r} = [r_0, \cdots, r_{N-1}]^T$. Linear interpolation is implemented to estimate channel coefficients between hybrid SC-OFDM blocks. Note that since the ZC sequence in (4) used for the pilot symbols is a constant modulus sequence, choices of P_Z do not affect the channel estimation performance under the estimation method considered in this letter. We consider Rayleigh frequency selective fading channels with $M = \{1, 2, 4, 16\}$ with the normalized Doppler frequency $f_D T_S = 5.4 \times 10^{-3}$. In the simulation, we assume that nonlinearity due to a power amplifier is not present at the transmitter. The BER performance is plotted for different values of average signal to noise ratio (SNR) per symbol E_s/σ_w^2, where E_s indicates the energy per symbol. To make a fair performance comparison, SNR per symbol for the proposed scheme is set as $E_s/\sigma_w^2 \cdot (1-\eta)$. From Fig. 7, it is confirmed that insertion of anchor symbols does not affect the BER performance of the proposed method.

IV. Conclusion

A novel out-of-band suppression method has been proposed in this letter. The experimental and simulation results have demonstrated that the proposed method suppresses the out-of-band leakage and imposes no BER performance penalty.

V. Acknowledgment

The authors would like to thank Dr. I. Chiba, Dr. M. Miyazaki, K. Ishioka, Y. Kato, K. Suzuki, H. Iura and K. Tsukamoto of Mitsubishi Electric Corporation for their encouragement and support throughout this work.

References

[1] N. Benvenuto, R. Dinis, D. D. Falconer, and S. Tomasin, "Single carrier modulation with nonlinear frequency domain equalization: An idea whose time has come - again," *Proc. IEEE*, vol. 98, no. 1, pp. 69–96, 2010.

[2] J. van de Beek and F. Berggren, "Out-of-band power suppression in OFDM," *IEEE Commun. Lett.*, vol. 12, no. 9, pp. 609–611, 2008.

[3] M. Faulkner, "The effect of filtering on the performance of OFDM systems," *IEEE Trans. Veh. Technol.*, vol. 49, no. 5, pp. 1877–1884, 2000.

[4] C. Ciochina-Duchesne, D. Castelain, and A. Bouttier, "Satellite profile in DVB-NGH," in *Proc. 6th Advanced Satellite Multimedia Systems Conference*, 2012, pp. 182–188.

[5] B. Porat, *A Course in Digital Signal Processing*. New York, NY, USA: John Wiley & Sons, 1997.

[6] C. Ciochina, F. Buda, and H. Sari, "An analysis of OFDM peak power reduction techniques for WiMAX systems," in *Proc. ICC 2006*, vol. 10, 2006, pp. 4676–4681.